

Defects dynamics during ageing cycles of InGaN blue light-emitting diodes revealed by evolution of external quantum efficiency - current dependence

Yue Lin,^{1,*} Yong Zhang,² Ziquan Guo,¹ Jihong Zhang,¹ Weilin Huang,¹ Yi-Jun Lu,¹ Zhonghua Deng,³ Zhuguang Liu,³ and Yongge Cao^{4,5}

¹Department of Electronic Science and Fujian Engineering Research Center for Solid-State Lighting, Xiamen University, Xiamen, Fujian 361005, China

²Electrical and Computer Engineering Department, University of North Carolina at Charlotte, Charlotte, North Carolina 28223, USA

³Fujian Institute of Research on the Structure of Matter, Chinese Academy of Sciences, Fuzhou, Fujian, 350002, China

⁴Beijing Key Laboratory of Opto-electronic Functional Materials & Micro-nano Devices, Department of Physics, Renmin University of China, Beijing, 100872, China

⁵Caoyongge@fjirsm.ac.cn

*Yue.Lin@xmu.edu.cn

Abstract: We report in detail the defect dynamics in the active region by monitoring the external quantum efficiency (EQE) – injection current curves, I-V curves, and electroluminescence spectra during the ageing test, under a forward current of 850 mA (85 A/cm²), room temperature. We apply a two-level model to analyze the EQE curves and the electroluminescence spectra. The results suggest that high injection density during the ageing may reduce the density of the Shockley-Reed-Hall nonradiative recombination centers and enhance the carrier mobility and diffusion length. The former effect would directly lead to initial surge of EQE, whereas the latter would enhance the effect of extended defects which leads to reduction in peak EQE and increase in EQE droop rate.

©2015 Optical Society of America

OCIS codes: (230.3670) Light-emitting diodes; (230.5590) Quantum-well, -wire and -dot devices.

References and links

1. J. Cho, E. F. Schubert, and J. K. Kim, "Efficiency droop in light-emitting diodes: Challenges and countermeasures," *Laser Photonics Rev.* **7**(3), 408–421 (2013).
2. M. H. Chang, D. Das, P. V. Varde, and M. Pecht, "Light emitting diodes reliability review," *Microelectron. Reliab.* **52**(5), 762–782 (2012).
3. Z. Q. Liu, T. B. Wei, E. Q. Guo, X. Y. Yi, L. C. Wang, J. X. Wang, G. H. Wang, Y. Shi, I. Ferguson, and J. M. Li, "Efficiency droop in InGaN/GaN multiple-quantum-well blue light-emitting diodes grown on free-standing GaN substrate," *Appl. Phys. Lett.* **99**(9), 091104 (2011).
4. J. Iveland, L. Martinelli, J. Peretti, J. S. Speck, and C. Weisbuch, "Direct measurement of Auger electrons emitted from a semiconductor light-emitting diode under electrical injection: identification of the dominant mechanism for efficiency droop," *Phys. Rev. Lett.* **110**(17), 177406 (2013).
5. J. I. Shim, D. P. Han, H. Kim, D. S. Shin, G. B. Lin, D. S. Meyaard, Q. F. Shan, J. Cho, E. F. Schubert, H. Shim, and C. Sone, "Efficiency droop in AlGaInP and GaInN light-emitting diodes," *Appl. Phys. Lett.* **100**(11), 111106 (2012).
6. B. J. Ahn, T. S. Kim, Y. Q. Dong, M. T. Hong, J. H. Song, J. H. Song, H. K. Yuh, S. C. Choi, D. K. Bae, and Y. Moon, "Experimental determination of current spill-over and its effect on the efficiency droop in InGaN/GaN blue-light-emitting-diodes," *Appl. Phys. Lett.* **100**(3), 031905 (2012).
7. S. Hwang, W. J. Ha, J. K. Kim, J. R. Xu, J. Cho, and E. F. Schubert, "Promotion of hole injection enabled by GaInN/GaN light-emitting triodes and its effect on the efficiency droop," *Appl. Phys. Lett.* **99**(18), 181115 (2011).

8. H. J. Li, J. J. Kang, P. P. Li, J. Ma, H. Wang, M. Liang, Z. C. Li, J. Li, X. Y. Yi, and G. H. Wang, "Enhanced performance of GaN based light-emitting diodes with a low temperature p-GaN hole injection layer," *Appl. Phys. Lett.* **102**(1), 011105 (2013).
9. L. C. Le, D. G. Zhao, D. S. Jiang, L. Li, L. L. Wu, P. Chen, Z. S. Liu, J. Yang, X. J. Li, X. G. He, J. J. Zhu, H. Wang, S. M. Zhang, and H. Yang, "Effect of V-defects on the performance deterioration of InGaN/GaN multiple-quantum-well light-emitting diodes with varying barrier layer thickness," *J. Appl. Phys.* **114**(14), 143706 (2013).
10. N. I. Bochkareva, Y. T. Rebane, and Y. G. Shreter, "Efficiency droop and incomplete carrier localization in InGaN/GaN quantum well light-emitting diodes," *Appl. Phys. Lett.* **103**(19), 191101 (2013).
11. Y. Lin, Y. Zhang, Z. Liu, L. Su, J. Zhang, T. Wei, and Z. Chen, "Spatially resolved study of quantum efficiency droop in InGaN light-emitting diodes," *Appl. Phys. Lett.* **101**(25), 252103 (2012).
12. Y. Lin, Y. Zhang, Z. Liu, L. Su, J. Zhang, T. Wei, and Z. Chen, "Interplay of point defects, extended defects, and carrier localization in the efficiency droop of InGaN quantum wells light-emitting diodes investigated using spatially resolved electroluminescence and photoluminescence," *J. Appl. Phys.* **115**(2), 023103 (2014).
13. X. A. Cao, P. M. Sandvik, S. F. LeBoeuf, and S. D. Arthur, "Defect generation in InGaN/GaN light-emitting diodes under forward and reverse electrical stresses," *Microelectron. Reliab.* **43**(12), 1987–1991 (2003).
14. F. Rossi, M. Pavesi, M. Meneghini, G. Salviati, M. Manfredi, G. Meneghesso, A. Castaldini, A. Cavallini, L. Rigutti, U. Strass, U. Zehnder, and E. Zanoni, "Influence of short-term low current dc ageing on the electrical and optical properties of InGaN blue light-emitting diodes," *J. Appl. Phys.* **99**(5), 053104 (2006).
15. L. Liu, M. Ling, J. Yang, W. Xiong, W. Jia, and G. Wang, "Efficiency degradation behaviors of current/thermal co-stressed GaN-based blue light emitting diodes with vertical-structure," *J. Appl. Phys.* **99**(5), 053104 (2006).
16. T. T. Chen, C. P. Wang, H. K. Fu, P. T. Chou, and S. P. Ying, "Electroluminescence enhancement in InGaN light-emitting diode during the electrical stressing process," *Opt. Express* **22**(S5), A1328–A1333 (2014).
17. O. Pursiainen, N. Linder, A. Jaeger, R. Oberschmid, and K. Streubel, "Identification of ageing mechanisms in the optical and electrical characteristics of light-emitting diodes," *Appl. Phys. Lett.* **79**(18), 2895–2897 (2001).
18. K. C. Yung, H. Liem, H. S. Choy, and W. K. Lun, "Degradation mechanism beyond device self-heating in high power light-emitting diodes," *J. Appl. Phys.* **109**(9), 094509 (2011).
19. S. Sawyer, S. L. Rumyantsev, and M. S. Shur, "Degradation of AlGaIn-based ultraviolet light emitting diodes," *Solid-State Electron.* **52**(6), 968–972 (2008).
20. S. L. Chuang, A. Ishibashi, S. Kijima, N. Nakayama, M. Ukita, and S. Taniguchi, "Kinetic model for degradation of light-emitting diodes," *IEEE J. Quantum Electron.* **33**(6), 970–979 (1997).
21. S. Buso, G. Spiazzi, M. Meneghini, and G. Meneghesso, "Performance degradation of high-brightness light emitting diodes under DC and pulsed bias," *IEEE Trans. Device Mater. Reliab.* **8**(2), 312–322 (2008).
22. M. Meneghini, N. Trivellin, G. Meneghesso, K. Orita, S. Takigawa, T. Tanaka, D. Ueda, and E. Zanoni, "Recent results on the physical origin of the degradation of GaN-based LEDs and lasers," *Proc. SPIE* **7939**, 79390W (2011).
23. K. Köhler, T. Stephan, A. Perona, J. Wiegert, M. Maier, M. Kunzer, and J. Wagner, "Control of the Mg doping profile in III-N light-emitting diodes and its effect on the electroluminescence efficiency," *J. Appl. Phys.* **97**(10), 104914 (2005).
24. K. Harafuji and K. Kawamura, "Magnesium diffusion at dislocation in Wurtzite-Type GaN crystal," *Jpn. J. Appl. Phys.* **44**(9A), 6495–6504 (2005).
25. M. E. Zvanut, Y. Uprety, J. Dashdorj, M. Moseley, and W. A. Doolittle, "Passivation and activation of Mg acceptors in heavily doped GaN," *J. Appl. Phys.* **110**(4), 044508 (2011).
26. Y. Lin, Y. L. Gao, Y. J. Lu, L. H. Zhu, Y. Zhang, and Z. Chen, "Study of temperature sensitive optical parameters and junction temperature determination of light-emitting diodes," *Appl. Phys. Lett.* **100**(20), 202108 (2012).

1. Introduction

Though the GaN-based multiple quantum wells (MQWs) light-emitting diode (LED) have been undergoing a rapid improvement in brightness, as well as external quantum efficiency (EQE), it has two issues remain to be tackled — one is the decreasing in EQE with injection current density (J_f), namely "EQE droop" [1], and the other is the luminous degradation [2]. Both of them may have multiple mechanisms, and some are shared by the two issues. Defects growth, Ohmic contact degradation, and darkening in the encapsulation can quench the luminous intensity slowly. Several mechanisms have been considered to be responsible for the EQE droop, such as Auger recombination [3, 4], electron leakages [5, 6], insufficient hole injection [7, 8], and defect-related mechanisms [9–12]. In our recent work, we associated the EQE droop with extended defects (EDs). As J_f increases, point defects (PDs) levels that initially act as nonradiative recombination centers by capturing the carriers will gradually be saturated, corresponding to the rising part of the EQE- J_f curve; while at high J_f , mobile carriers free from energy fluctuations will be captured by EDs, leading to EQE droop [11,

12]. Therefore we believe that there exist some connections between EQE droop and luminous degradation: the evolution of defects in the device, which has proved to be one of many ramifications of high forward current and temperature stress [13, 14]. Hence, as different types of defects are generated during the ageing, along with the luminous degradation, the EQE- J_f curves are shifting slowly. That helps us to evaluate the defect-dynamics which in turn enriches the theoretical basis of LEDs lifespan prediction for industry needs. However, because these two topics traditionally were investigated separately, only a few works seen in the literature hitherto focusing on the evolution of the EQE curve with ageing [14–17].

In this work, we investigate the changes in the EQE curves, I-V curves and EL spectra during a high-current-stress ageing test. The initial rise in the low-current EQE, in conjunction with changes in the forward voltage in the same period, indicates that high current stress reduces the density of PDs where the undesirable Shockley-Reed-Hall (SRH) recombination takes place, and therefore enhances the carrier densities as well as its mobility and diffusion length, which are further supported by the accompanying blue-shift in ELs with ageing time. At higher injection density, the rise in carrier mobility leads to the fact that more carriers are captured by EDs, and therefore higher EQE droop rates.

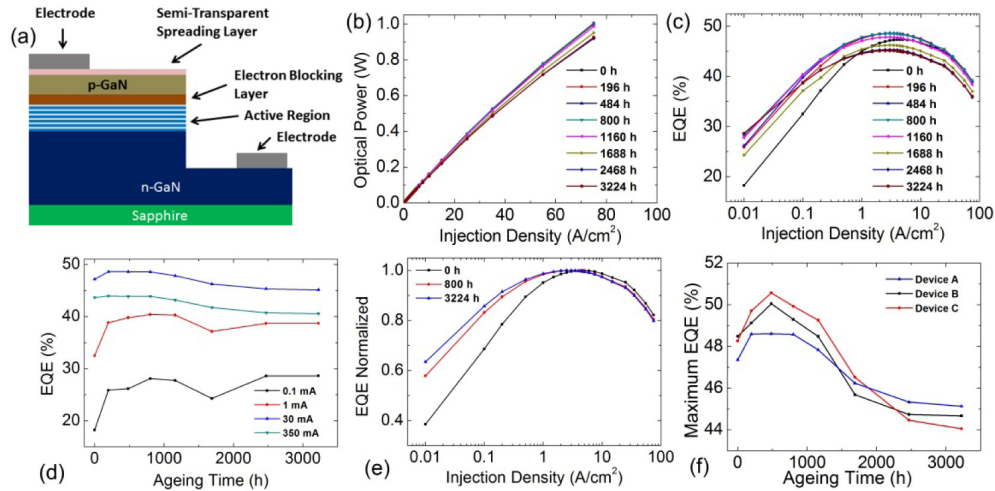


Fig. 1. (a) A schematic of the structure of the devices under test; (b) Plots of optical power vs. J_f and (c) EQE curves at different ageing times for Device A; (d) The EQE measured at different J_f over the ageing test; (e) 3 normalized EQE curves of Device A at different ageing times; (f) The maximum EQEs vs. ageing time for 3 devices.

2. Experimental setup

We employed InGaN/GaN MQW LEDs with similar structures to the device of sapphire substrate in [12], where we performed spatially resolved EQE study. The structure of these devices employed in this work is illustrated in Fig. 1(a). The chips in the devices were 1 mm^2 in size. To avoid the influence from encapsulations, we removed them when measuring the optical parameters, and covered them back before send the devices to ageing. We subjected 7 these devices to direct current stress on $I_f = 850 \text{ mA}$, corresponding to $J_f = 85 \text{ A/cm}^2$, at room temperature ($\sim 300 \text{ K}$). We measured the EQE curves with I_f ranging from 0.1 to 750 mA ($J_f = 0.01\text{-}75 \text{ A/cm}^2$), along with the related EL spectra and different forward voltages (V_f). These measurements were carried out before ageing (denoted as 0 h) and at 7 time points of ageing: $196, 484, 800, 1160, 1688, 2468$ and 3224 h . The optical parameters were measured by a Spectro320 (Instrument Systems Inc., Germany), and Keithley 2400 and 2510 (Keithley

Instruments Inc., USA) served as electrical multimeter and temperature controller, respectively.

3. Results and discussions

From the optical power and forward current we are able to calculate the EQE, which is defined as the ratio between the number of photons emitted per second, n_{hv} , and the number of electrons injected into active region per second, n_e , by using the Eq. (1) below.

$$\eta_{EQE} = \frac{n_{hv}}{n_e} = \frac{\int_{E(h\nu)>0} \frac{E(h\nu)}{h\nu} d(h\nu)}{(I_f/q)} \quad (1)$$

In the numerator of the right-hand side of Eq. (1), the $E(h\nu)$ denotes the optical power spectrum and, when divided by $h\nu$, would give the number of photons with energy of $h\nu$ emitted per second, and the integral sums over the spectral region where $E(h\nu) > 0$, would give n_{hv} ; The denominator, where I_f and q denote the forward current and elementary charge respectively, gives n_e . During ageing, all the devices exhibited very similar behaviors in optical and electrical parameters. For one of these devices (Device A), the curves of optical power vs. J_f are illustrated in Fig. 1(b) and the EQE curves are shown in Fig. 1(c), which all indicate that the curve is shifting with varying ageing time (τ_a). Interestingly the lowest EQE at 0.01 A/cm² occurs at 0 h. Shown in Fig. 1(d) are curves of EQE vs. ageing time for four selected current levels from low to high. All of them show initial increases with ageing, although by different degrees. The improvement for the lower current portion is more significant and the EQE saturates at around 200 h, and remains more or less the same afterward; whereas for the higher current portion the improvement is less significant and the EQE decreases after ~200 h. These observations can be seen more clearly from the normalized EQE vs. ageing time curves shown in Fig. 1(e) for different ageing stages: fresh, mid-term, and long-term, respectively. Ageing improves the low current EQE, but at high current it leads to lower EQEs as well as higher droop rates. Figure 1(f) shows that the maximum EQE vs. ageing time for 3 devices, exhibiting non-monotonic behavior with peaks at $\tau_a = \sim 500$ h. Our ageing data for high current contradict to most of the previous reports where monotonic darkening at high current was observed with ageing [18–22]. There are nonetheless some literature reported the similar initial intensity increase [15–17]. Noting that the EQE curves are determined largely by interplays between radiative and nonradiative recombination of the carriers, we analyze the rising part using a two-level model [11]. The rising part of the EQE curve can be described by Eq. (2).

$$\eta_{EQE} = \frac{C}{2} \left[1 - \frac{\alpha + \beta}{J_f} + \sqrt{\frac{4\alpha}{J_f} + \left(1 - \frac{\alpha + \beta}{J_f} \right)^2} \right] \quad (2)$$

In Eq. (2), C is a constant depending on the light extraction rate of the device; $\alpha = W_r W_t / \gamma_t$, $\beta = N_t W_t$, where W_r and W_t denote the inter-band radiative recombination rate and nonradiative recombination rate via PDs, respectively; γ_t the defect capture rate; N_t the density of defect states. In the low current region, because of the low carrier mobility due to energy band fluctuation, the most relevant nonradiative recombination centers are uniformly distributed PDs. Note that $N_t = 0$ thus $\beta = 0$ yields $\eta_{EQE} / C = 1$, indicating 100% internal quantum efficiency (η_{IQE}). Equation (2) fits the experimental data exceptionally well (with all

R-squares exceed 0.995), and examples are presented in Fig. 2(a). The extracted values for α and β vs. τ_a are shown in Fig. 2(b) for Device A.

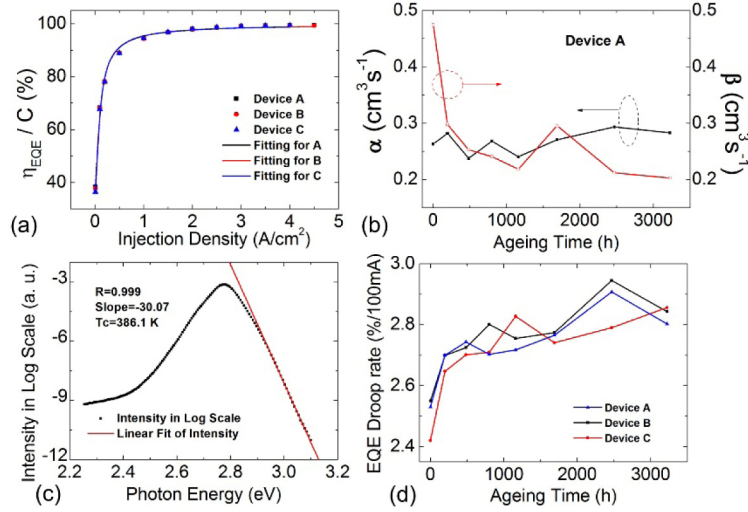


Fig. 2. (a) Examples of the two-level model curve fittings. dots: data measured, lines: fitting curves; (b) Changes in α (black) and β (red) respectively with ageing time; (c) The linear fitting (red line) of the high-energy slope of the EL intensity in log scale (black dots) on $I_f = 850$ mA, the result indicates that the carrier temperature during ageing is ~ 386 K; (d) The EQE droop rates for 3 devices over the entire ageing test.

We find that β decreases significantly with increasing ageing time, in particular very rapidly in the initial 196 h, but α remains more or less the same, suggesting that ageing has resulted in reduction of N_t or the number of nonradiative recombination centers. This finding further suggests that high injection current can modify some PDs, and makes them either diminish or become benign. In the literature, this initial EQE surge was ascribed to Mg dopant activation, including breaking the Mg-H bonds in the p-GaN [15]. However, we argue that this is not necessarily true. As reported, the Mg dopant activation mostly occurs at high temperature annealing during fabrication, usually in the atmosphere consisting of pure oxygen, at the temperature ranging from 1000 to 1300 K [23–25]. Our EL spectra took during ageing, for example a typical one shown in Fig. 2(c) at 850 mA, indicates that the electron temperature, which is typically higher than the lattice temperature, did not exceed 400 K, thus was significantly lower than the minimum requirement of ~ 798 K (525 °C) for inducing dopant activation [25]. Therefore, the Mg activation is unlikely to occur at such low temperature. The reduction in non-radiative SRH centers also results in increases in the carrier mobility, leading to longer diffusion length. It increases the probability of the electron-hole pairs being susceptible to the EDs, which serves as a kind of non-radiative recombination centers at higher current and would intensify the EQE droop. Therefore, in addition to the raising part of the EQE curve, we also investigate the droop rate δ for the falling part, which is defined as

$$\delta(I) = \frac{\eta_{\max} - \eta_I}{\eta_{\max} \times (I - I_{\max})} \times 100\% \quad (3)$$

In Eq. (3), the η_{\max} denotes the maximum EQE in the EQE curve; η_I the EQE at $I_f = I$; I_{\max} the I_f at which the EQE reaches the maximum. Taking $I = 750$ mA, we evaluate the droop rate as a function of ageing time, as shown in Fig. 2(d), which exhibits almost inverse trends with respect to β in the Figure 2(b). The initial increase in droop rate should not be viewed as a

negative effect on the device performance. As shown in Fig. 1(d) and Fig. 1(f), the peak EQE increases and the high current EQE remains nearly the same in the early stage of ageing, which results an increase in the droop rate. The increase in the peak EQE is due to the reduction in SRH recombination, as explained earlier. However, the slow increase in EQE droop rate afterward is due to a different mechanism. The decrease in PDs leads to longer diffusion lengths for carriers, which raise the probability of their being captured by EDs, resulting in less growth or even decrease of EQEs at higher injection density. The fact that the increase in carrier mobility enlarges the impact area of each ED is responsible for the slow increase in EQE droop rate with ageing time.

To find further evidence for the reduction in SRH centers and increase in carrier mobility, we also investigated the I-V curve and EL spectra. We could fit all the I-V curves with a rearranged Shockley Function given as Eq. (4) and obtained the series resistance R_s .

$$V_f = \frac{nkT}{q} \ln\left(\frac{I_f}{I_0}\right) + I_f R_s \quad (4)$$

In Eq. (4), the n denotes the ideality factor; q the elementary charge; I_0 the reverse saturation current; and R_s the series resistance. The total R_s is the sum of resistance of several parts, such as Ohmic contact, the active region, and gold wires. The Ohmic contact contributes a majority part especially at higher current. The R_s vs. τ_a is plotted in Fig. 3(a), which shows a continued increase in R_s , due to the degradation in the Ohmic contact.

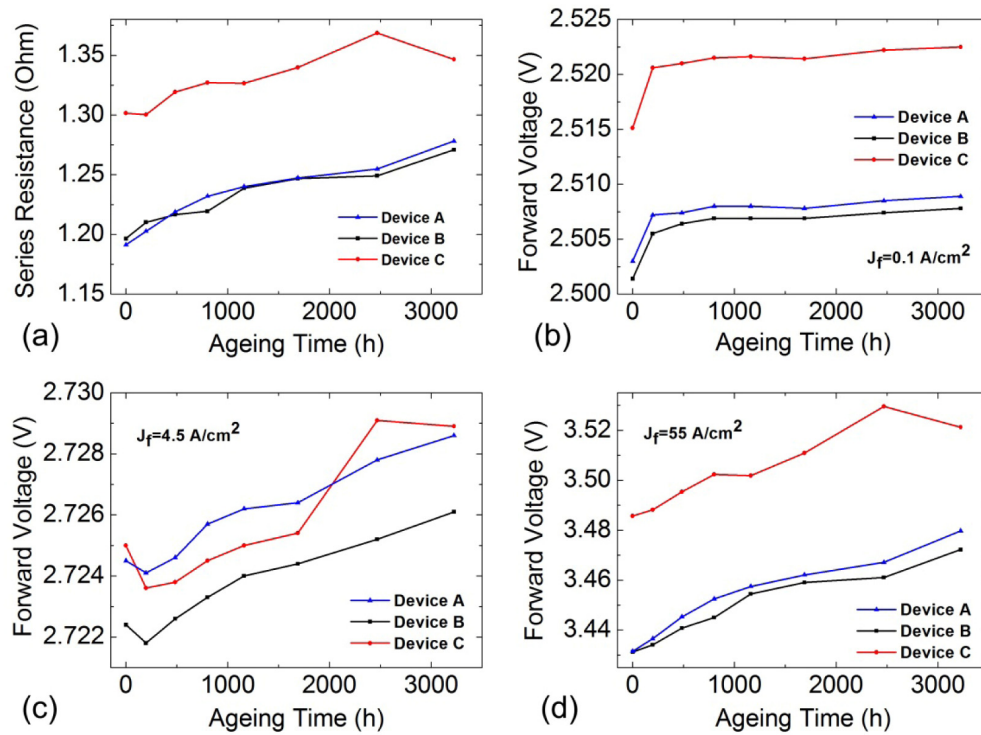


Fig. 3. (a) Series resistances vs. τ_a for 3 devices, and their forward voltages vs. τ_a at J_f of (b) 0.1 A/cm² of Region #1, (c) 4.5 A/cm² of Region #2 and (d) 55 A/cm² of Region #3.

Note that the rise in resistance of Ohmic contact will not directly affect EQE but does affect energy or luminous efficiency, because the device is driven by a current source, therefore the increase in R_s only results in increase of V_f but would not reduce the current

injection into the active region. The connection between the resistance of the active region and the EQE will be discussed later. We also compare the V_f vs. ageing time under a constant J_f over the entire ageing test, discovering 3 J_f regions with different behaviors of V_f . Typical V_f vs. τ_a plots of region #1 ($J_f < \sim 1.5$ A/cm²), #2 (~ 1.5 A/cm² $< J_f < \sim 15$ A/cm²) and #3 ($J_f > \sim 15$ A/cm²) are illustrated in Figs. 3(b)-(d) for typical J_f , respectively. In Region #1, the V_f experiences a rapid increase by ~ 5 mV in the initial 196 h, followed by a slower growing, resembling the black and red lines in Fig. 1(d); In Region #2, the V_f first decreases by ~ 1 mV and rises as it does in Region #1, but at a higher rate; and in Region #3, it increases monotonically at the highest rate. The “expected” increases in Region #1 and #2 after 196 h and the entire Region #3 can be ascribed to the increase in R_s , while mechanisms of “unusual” behaviors in the initial parts of the first two Regions are interpreted below. In Region #1, where the J_f is very low, there always exist ubiquitously distributed local deep PDs levels that enhance the nonradiative SRH recombination and cause parallel tunneling electron leakage which effectively draws down the V_f . After ageing, the reduction in the effective PD concentration effectively increases the resistance of the active region and thus reduces the current for the same V_f , reflecting as the rise in V_f and EQE. It resembles the rise in the shunt resistance. Whereas in Region #2 with moderate J_f , the enhance in carrier mobility would then manifest itself as reduction in resistance of the active region, resulting the falling of V_f within 196 h. Such effect is so weak that soon neutralized by the Ohmic contact degradation, resulting in the following V_f increase.

To study the change in EL spectra, we first define a High to Low (H-L) ratio ζ_{H-L} , which is the ratio between integrated EL intensities, P_H and P_L , with photon energy larger and lower than the peak energy:

$$\zeta_{H-L} = \frac{P_H}{P_L} = \frac{\int I_{High}(E)d(E)}{\int I_{Low}(E)d(E)} \quad (5)$$

The physical meanings of these parameters are illustrated in Fig. 4(a). The red and blue region denote the low and high energy parts, respectively. The peak energy can be taken as an approximate for the mobility edge of the carriers. It is found that for all the devices, the EL spectra all exhibit slight blue-shifts as a whole as well as the peak energy, so ζ_{H-L} increases as the ageing goes on, as shown by the black line in Fig. 4(b). Because the changes in ζ_{H-L} bear high resemblance to the shift in peak energy, as shown in Fig. 4(b), such blue-shift is resulted from a distortion in the spectrum shape, rather than simply a spectrum shift towards shorter wavelengths as a whole, which means that ageing increases the radiative recombination from more mobile carriers, and at the same time, reduces that from localized states. Note that the line-widths of the spectra do not increase significantly, therefore the effect of junction temperature change on the spectra could be ignored [26].

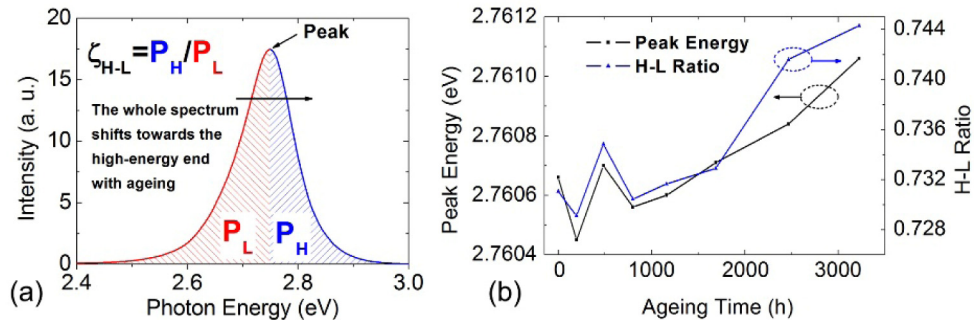


Fig. 4. (a) Definition of H-L Ratio, the P_L and P_H are the areas below the low and high energy side respectively; (b) The shift in peak energy (black) and ζ_{H-L} (blue) with the ageing time.

The seemingly small shift in the EL spectrum is a subtle effect that would normally be unnoticed. However, the consistency in the trend and among multiple devices indicates that it is a real effect. The loss of emission on the low energy side indicates a change in the energy landscape, possibly alternations in QW width or In composition fluctuations. It further supports the suggestion that ageing improves the carrier mobility, which in turn increases or decreases the peak EQE due to the interplay between the PDs and EDs at different ageing stages.

4. Conclusion

In summary, with varying ageing time, the high current-stress leads to improvement in EQE at low current throughout the ageing time, initial increase then decrease in the peak EQE, and similar variation but to less extent for the high current region. The experimental results suggest that the PDs may be partly removed by short period of high-current stress, which in consequence could improve the carrier mobility. On one hand, this could increase the EQE at low injection because of less undesirable nonradiative centers; on the other hand, the increase in diffusion length of carriers could make it easier for them to be captured by EDs far away from where they generate, which would result in severer EQE droop at high injections. We need to further confirm these assumptions by carrying out more kinds of measurements, such as low-temperature photoluminescence and ELs, during new rounds of aging in the future. In addition, first-principle researches are expected for improving the solidity of theoretical basis.

Acknowledgments

The work at Xiamen University was supported by the 863 project of China under Grant 2013AA03A107, Major Science and Technology Project between University-Industry Cooperation in Fujian Province under Grant No. 2013H6024, and Key Project of Fujian Province under Grant No. 2012H0039; at UNC-Charlotte was supported by MURI program (under supervision of Dr. William Clark) from the U.S. Army Research Laboratory and the U.S. Army Research Office under grant number Army W911NF-10-1-0524, and Bissell Distinguished Professorship. Dr. Yue Lin thanks Miss Julian B. Su for proof-reading.